ACS AUTHORCHOICE

Article

Environmental Science & Technology

Cite This: Environ. Sci. Technol. 2018, 52, 7259−7268

pubs.acs.org/est

High Permeation Rates in Liposome Systems Explain Rapid Glyphosate Biodegradation Associated with Strong Isotope Fractionation

Benno N. Ehrl,[†] Emmanuel O. Mogusu,[†,¶] Kyoungtea Kim,[‡] Heike Hofstetter,[§] Joel A. Pedersen,*[,‡,§,∥] and Martin Elsner*[,†,⊥]

[†]Institute of Groundwater Ecology, Helmholtz Zentrum München, Ingolstädter Landstrasse 1, 85764 Neuherberg, Germany

[¶]Department of Chemistry, Mwenge Catholic University, P.O. Box 1226, Moshi, Tanzania

[‡]Molecular and Environmental Toxicology Center, University of Wisconsin, Madison, Wisconsin 53706, United States

[§]Department of Chemistry, University of Wisconsin, Madison, Wisconsin 53706, United States

[∥]Departments of Soil Science and Civil & Environmental Chemistry, University of Wisconsin, Madison, Wisconsin 53706, United States

[⊥]Institute of Hydrochemistry, Chair for Analytical Chemistry and Water Chemistry, Technical University of Munich, Marchioninistrasse 17, 81377 Munich, Germany

Supporting Information

ABSTRACT: Bacterial uptake of charged organic pollutants such as the widely used herbicide glyphosate is typically attributed to active transporters, whereas passive membrane permeation as an uptake pathway is usually neglected. For 1-palmitoyl-2-oleoyl-*sn*-glycero-3-phosphocholine (POPC) liposomes, the pH-dependent apparent membrane permeation coefficients (P_{app}) of glyphosate, determined by nuclear magnetic resonance (NMR) spectroscopy, varied from P_{app} (pH 7.0) = 3.7 (±0.3) × 10^{-7} m·s^{-1} to P_{app} (pH 4.1) = 4.2 (±0.1) × 10^{-6} m·s^{-1}. The magnitude of this surprisingly rapid membrane permeation depended on glyphosate speciation and was, at circumneutral pH, in the range of polar, noncharged molecules. These findings point to passive membrane permeation as a potential uptake pathway during glyphosate biodegradation. To test this hypothesis, a Gram-negative glyphosate degrader, *Ochrobactrum sp*. FrEM, was isolated from glyphosate-treated soil and glyphosate permeation rates inferred from the liposome model system were compared to bacterial degradation rates. Estimated maximum permeation rates were, indeed, 2 orders of magnitude higher than degradation rates of glyphosate. In addition, biodegradation of millimolar glyphosate concentrations gave rise to pronounced carbon isotope fractionation with an apparent kinetic isotope effect, $AKIE_{carbon}$, of 1.014 ± 0.003. This value lies in the range typical of non-masked enzymatic isotope fractionation demonstrating that glyphosate biodegradation was not subject to mass transfer limitations and glyphosate exchange across the cell membrane was rapid relative to enzymatic turnover.

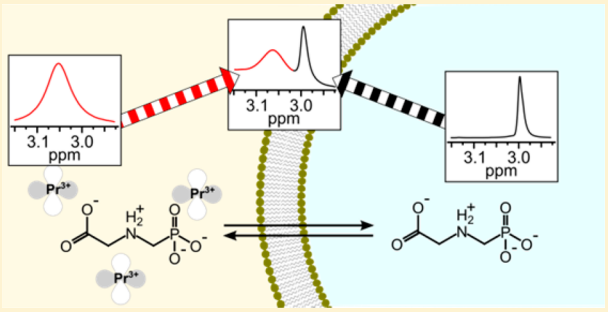

INTRODUCTION

Glyphosate (*N*-(phopshomethyl)glycine) is a nonselective, systemic, postemergent herbicide widely used in agriculture because of its ability to effectively control a broad range of weeds.[1−3] One component of its success has been the introduction of transgenic, glyphosate-resistant crops.[4,5] The worldwide market share of glyphosate is estimated at USD 5.6 billion, with the USGS estimating glyphosate use at more than 130 000 tons in 2015 alone in the USA.[2,6,7] Historically, the acute toxicity of glyphosate has been considered low,[3] it appears, however, that the impact of glyphosate on the environment has been underestimated.[8−10] Most importantly, the ubiquitous use of glyphosate has been found to affect biodiversity,[11] which is aggravated by increased usage due to the planting of glyphosate-resistant crops.[12,13] The effect of glyphosate on human health is currently disputed. After the World Health Organization classified glyphosate as "probably carcinogenic" to humans (Group 2A),[14] discussion has continued on whether or not glyphosate use poses a cancer risk.[15,16] In addition, the detection of glyphosate and its metabolite aminomethylphosphonic acid (AMPA) in surface waters and groundwaters at increasing frequencies lends urgency to the need to more thoroughly explore its environmental fate.[17−19] In particular, an improved understanding is warranted on the key drivers that limit its natural

Received: February 21, 2018
Revised: May 17, 2018
Accepted: May 23, 2018
Published: May 23, 2018

DOI: 10.1021/acs.est.8b01004
Environ. Sci. Technol. 2018, 52, 7259−7268

microbial degradation, because biodegradation represents the most effective glyphosate remediation pathway.[20−23]

A series of publications highlights the particular role of pollutant mass transfer into microbial cells as a rate-limiting step for biodegradation, especially at low pollutant concentrations.[24,25] The mass transfer of polar and charged species (e.g., zwitterionic glyphosate[26]) into bacterial cells is currently assumed to occur by active transport.[27,28] The passive permeation of charged organic molecules across cell membranes is less well understood than that of neutral nonpolar organic pollutants.[29,30] The extent to which the diffusion barrier imposed by the bacterial membrane constitutes an even stronger bioavailability limitation for these charged molecules than for noncharged pollutants is poorly understood.[31] Thus, it is important not only to investigate the membrane permeation rate but also to identify whether the rate of glyphosate is determined by the enzymatic reaction or by slow mass transfer of the herbicide across the cell envelope[28,32] (where mass transfer can occur by either membrane permeation[31] or active transport[33]).

To investigate membrane permeation processes, a variety of model systems have been used to study the diffusion of drugs and cosmetic ingredients through human epithelia, ranging from *n*-octanol−water partitioning to more complex systems such as lipid discs and planar lipid membranes.[34,−38] However, these model systems are often composed of non-natural lipids, contain organic solvents, or present non-natural lipid−water interfaces. Therefore, membranes resembling biological lipid bilayers (e.g., liposomes with natural lipid composition) are currently the best model to approximate permeation rates valid for natural systems.[39,40] Here, we used unilamellar liposomes composed of a single zwitterionic phospholipid, 1-palmitoyl-2-oleoyl-*sn*-glycero-3-phosphocholine (POPC), as a simplified system to investigate the permeation of glyphosate across phospholipid bilayers.[41] The POPC vesicles have a gel-to-liquid crystalline phase transition temperature of −2 °C and, under our experimental condition, are in the liquid crystalline phase, resembling the dominant state of membranes of many bacteria.[42,43] This model system lacked additional membrane constituents (e.g., anionic lipids, proteins, lipopolysaccharides) and cell envelope structures (phase-segregated domains in membranes, double membrane in Gram-negative bacteria, peptidoglycan cell wall) that are present in bacterial cells.[44] We note that porins in the Gram-negative bacterial outer membrane permit passage of hydrophilic molecules with molecular masses $\lesssim$600 Da[29] and the large pores of peptidoglycan do not restrict pollutant permeation.[45]

Permeation of the phospholipid bilayer leads to chemical exchange between the outside and the inside of the liposomes. Nuclear magnetic resonance (NMR) spectroscopy offers a direct approach to quantify the permeation process based on the following principle. A nucleus gives rise to an NMR signal at a chemical shift that reflects its chemical environment. Liposomes prepared and suspended in the same solution have roughly equivalent chemical environments inside and outside the liposome. Addition of a non-permeable chemical shift agent (such as a lanthanide ion) to the solution either interior or exterior to the liposome alters the chemical environment inside vis-à-vis outside the liposome (as the shift agent cannot cross the lipid bilayer) and results in distinct peaks in the NMR spectrum for the nucleus inside and outside the liposomes.[37,41,46] (In the present study, praseodymium(III) ions (Pr^{3+}) were added to the solution external to the liposomes as a non-permeating chemical shift agent.) When the apparent exchange rate constant (k_{tr}) between the two chemical environments (here, inside and outside the liposomes) is smaller than the observed frequency difference between the two states ($\Delta\upsilon$), dynamic exchange of nuclei between chemical environments at equilibrium leads to line broadening.[47] Lineshape analysis subsequently allows quantification of chemical exchange between the two environments based on the evaluation of associated line broadening in the NMR spectrum.[47]

Complementary to these model systems, we recently advanced compound-specific isotope analysis (CSIA) as an analytical approach to trace limitations of mass transfer across the cell envelope directly in vivo while pollutant biodegradation is ongoing.[25,31] The underlying principle is the kinetic isotope effect of the associated enzymatic reaction. As the activation energy during a biochemical reaction is higher for bonds containing a heavy isotope, the turnover of molecules with a heavy isotope in the reactive position is slower. Therefore, as the enzymatic reaction proceeds, molecules containing heavy isotopes become enriched in the residual (nonreacted) substrate relative to those with light isotopes.[48] This trend can be evaluated by considering the change in the isotope ratio R_t relative to the initial isotope ratio at the beginning of the degradation R_0, and by relating it to the fraction of the remaining pollutant f according to the Rayleigh equation[49,50] (1)

$$\ln\left(\frac{R_t}{R_0}\right) = \ln\left(\frac{\delta^{13}C_t + 1}{\delta^{13}C_0 + 1}\right) = \varepsilon \cdot \ln(f) \tag{1}$$

where the enrichment factor ε describes how much slower heavy isotopes react compared to light isotopes. Here, the carbon isotope values $\delta^{13}C_t$ and $\delta^{13}C_0$ at time t and at the beginning of a reaction, respectively, are expressed relative to an international reference material $\delta^{13}C = (R_{Sample} - R_{Reference})/R_{Reference}$ to ensure comparability among laboratories. Thullner et al. delineated a new angle to use the change in isotope ratios as a diagnostic tool to directly observe mass-transfer limitation: strong isotope fractionation is observable, only if the pollutant exchange across the cell envelope is faster than its enzymatic turnover.[51] Otherwise, substrate molecules, which experience the isotopic discrimination during the enzymatic reaction in the cytosol, are used up completely so that they do not return to the bulk solution where the isotope ratio is assessed.[51−53] As a consequence, the enzymatic isotope fractionation that is observable in solution becomes masked in the presence of mass transfer limitations: i.e., when active transport (or passive membrane permeation) into and out of the cell is the rate-determining step in biodegradation.[25,33]

For this study, we used a combined approach to gain insight into the role of passive permeation for biodegradation of the zwitterionic pollutant glyphosate, which exists as either a net monoanion (pH < 6) or a net dianion (pH > 6) at circumneutral pH. First, an NMR study was conducted to experimentally determine pH-dependent passive membrane permeation of glyphosate in phosphatidylcholine liposomes as a model system. Second, passive permeation rates were extrapolated and compared to biodegradation rates of different glyphosate degraders to elucidate the role of passive membrane permeation of glyphosate for nutrient uptake. To this end, *Ochrobactrum sp.* FrEM, a new glyphosate degrader, was isolated from a vineyard soil treated with glyphosate,

DOI: 10.1021/acs.est.8b01004
Environ. Sci. Technol. 2018, 52, 7259−7268

characterized, and used for degradation experiments. The isotope fractionation measured during glyphosate biodegradation by *Ochrobactrum sp*. FrEM was explored as a diagnostic tool to directly observe the presence or absence of mass transfer limitations and, thus, to validate the assessment based on the results of the liposome model system and our theoretical considerations.

EXPERIMENTAL SECTION

Chemicals. A list of chemicals used can be found in the Supporting Information.

Liposome Preparation and Characterization. A 25 mg·mL^{-1} solution of 1-palmitoyl-2-oleoyl-*sn*-glycero-3-phosphocholine (POPC, transition temperature of −2 °C) in chloroform was prepared, and 50 mg of POPC (2 mL of the POPC solution) was added to a 3 mL screw cap glass vial tested prior to the experiment to withstand exposure to liquid nitrogen (see below). The chloroform was evaporated under a N_2 stream, and the lipid film was dried with vacuum for at least 12 h. The dried lipids were hydrated with 1 mL of 20 mM glyphosate in D_2O containing a small amount of 3-(trimethylsilyl)-2,2,3,3-tetradeuteropropionic acid (TSP) as internal reference for NMR. The pH of the solution, ranging from pH 4.1 to pH 7.8, was adjusted prior to hydration with 1 M sodium hydroxide (in D_2O). (Effective solvent suppression (vide infra) resulted in an insignificant increase in the HOD peak due to NaOH addition.) The vial was vortexed thoroughly; liposomes formed, and the suspension was subjected to three freeze−thaw cycles (freeze in liquid nitrogen for 5 min, thaw in 40 °C water bath for 5 min, and vortex for 30 s) followed by extrusion to yield unilamellar liposomes of uniform size distribution.[54,55] The liposomes were extruded in 1000 μL syringes with 11 passages through a 0.2 μm polycarbonate filter with an Avanti Mini-Extruder (Avanti Polar Lipids, Inc., USA). The hydrodynamic size and the zeta potential of the vesicles were determined by dynamic light scattering and laser Doppler electrophoresis with a ZetaSizer Nano ZS (Malvern Instruments Ltd., United Kingdom) in dilutions of 2 μL of liposome solution in 800 μL of D_2O. The temperature of the measurement cell was 25 °C. Ten measurements were averaged for each technical replicate (six replicates for dynamic light scattering and five replicates for laser Doppler electrophoresis).

Nuclear Magnetic Resonance Spectroscopy. All measurements were carried out on an Avance III 500 MHz spectrometer equipped with a BBFO+ smartprobe (Bruker, USA) at a sample temperature of 25 °C. NMR spectra were recorded with TopSpin 3.5.6 (Bruker, USA). Apodization, Fourier transformation, phase and baseline corrections, absolute referencing on TSP, spectral analysis, and peak fitting were carried out with MestReNova 11.0.3 (Mestrelab Research, Spain). Standard Bruker pulse sequences were used, and the spectra collection parameters are summarized in Table S1.

Assessing the Line Broadening Due to Chemical Exchange Across the Liposome Membrane. First, a standard ^{1}H spectrum of 550 μL of glyphosate liposome solution was collected to assess the pH-dependent chemical shift of the HOD peak, and the chemical shift of the phosphorus nucleus was determined with proton decoupling (^{31}P{^{1}H}). Then, a proton spectrum with phosphorus decoupling ^{1}H{^{31}P} and solvent suppression was recorded. We added 5.5 μL of a 50 mM $PrCl_3$ solution in D_2O to the NMR tube to a final concentration of 0.5 mM $PrCl_3$. Another

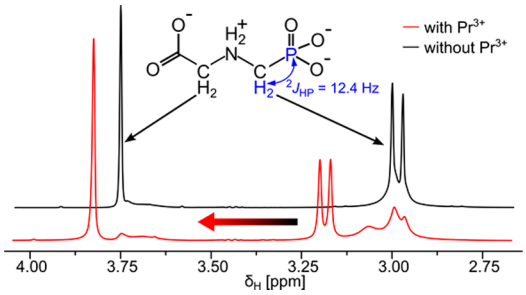

Figure 1. $^2J_{HP}$ coupling prevents direct measurement of glyphosate permeation of liposomes with standard ^{1}H-spectra. Glyphosate showed one singlet at 3.74 ppm and one doublet at 2.99 ppm in the ^{1}H NMR spectrum with solvent suppression (black line). Strong $^2J_{HP}$ coupling led to formation of a doublet centered at 2.99 ppm. Upon Pr^{3+} addition to the liposome suspension, the spectrum changed (red line). The glyphosate peaks outside the liposomes were shifted downfield (doublet at 3.2 ppm and singlet at 3.79 ppm), and the peaks inside the liposomes broadened due to chemical exchange. As a consequence, the individual doublet peaks overlapped, almost coalescing into a singlet and rendering peak shape analysis impossible. Both spectra in this figure were collected at pH 7.5.

^{1}H{^{31}P} spectrum with solvent suppression was recorded, and the glyphosate peaks prior to and after $PrCl_3$ addition were compared by fitting of the peaks. The strong $^2J_{HP}$ coupling of 12.4 Hz between the phosphorus and adjacent protons led to splitting of the peak at 2.99 ppm into a doublet in the ^{1}H NMR spectrum (Figure 1). This doublet, however, complicated peak shape analysis to quantify the rate of glyphosate permeation across liposomes. In the absence of Pr^{3+}, the shape of the separated doublet peaks could be fit. However, addition of Pr^{3+} led to line broadening due to chemical exchange between the inside and the outside of the liposomes. Thus, the individual peaks of the doublet signal overlapped with each other, rendering peak shape analysis unreliable. We therefore used a ^{1}H NMR pulse sequence that combined solvent suppression (watergate W5) with phosphorus decoupling. As a result, the doublet peak collapsed to a well-resolved singlet that was distinguishable from the POPC liposome signals (Figure 2A).

Bacterial Isolation and Characterization. For bacterial isolation from soil, mineral salt medium at pH 7.0 containing 60 mM sodium glutamate as carbon source and 38 mM ammonium chloride as nitrogen source was used. Glyphosate (3 mM) was the sole phosphorus source. A detailed description of the bacterial isolation from vineyard soil can be found in the Supporting Information.

Biodegradation of Glyphosate by *Ochrobactrum sp*. FrEM. The biodegradation of glyphosate by *Ochrobactrum sp*. FrEM was carried out in two biological replicates. We inoculated 50 mL of medium (see the Supporting Information) with *O. sp*. FrEM and incubated the culture at 30 °C at 160 rpm overnight. Cells were harvested by centrifugation (2100*g*, Heraeus Megafuge 1.0R, Germany), washed twice with medium, and transferred to 50 mL of fresh medium lacking phosphorus for phosphorus depletion. After incubation at 30 °C for 48 h, cells were harvested by centrifugation (2100*g*, Heraeus Megafuge 1.0R, Germany) and used to inoculate 150 mL of medium containing 120 μM glyphosate as the only phosphorus source. Bacterial growth was monitored at OD_{600} with a Cary 50 Bio UV−vis spectrometer (Varian Medical Systems, Inc., USA). During glyphosate biodegradation, samples for isotope analysis (10 mL) and the reaction was

DOI: 10.1021/acs.est.8b01004
Environ. Sci. Technol. 2018, 52, 7259−7268

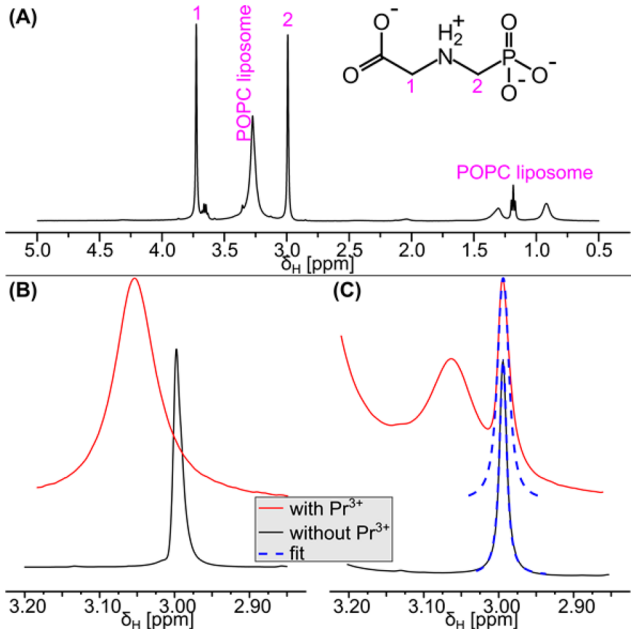

Figure 2. Line broadening due to exchange can be quantified by fitting the peaks in $^{1}H\{^{31}P\}$ NMR spectra. (A) Clear separation of the glyphosate signals from the signals of the POPC liposomes in the $^{1}H\{^{31}P\}$ NMR spectrum (black line) enabling reliable peak shape analysis. (B) Spectral region showing glyphosate protons attached to carbon 2 with (red line) and without (black line) Pr^{3+} in the absence of liposomes. The line broadening upon Pr^{3+} addition was caused by the interaction with the paramagnetic Pr^{3+}. Even though the signal without Pr^{3+} slightly overlapped with the broad glyphosate signal in the presence of Pr^{3+}, both peaks were well resolved. (C) The glyphosate peaks inside and outside the liposomes remained well resolved when POPC liposomes were present. Fitting the peak shape (blue dashed lines) prior to (black line) and after (red line) the addition of $PrCl_3$ yielded peak widths and, thus, allowed the line broadening to be quantified. The broadening of the glyphosate peak inside the liposomes (2.99 ppm) was caused by chemical exchange of glyphosate between the inside and the outside of the liposomes, because the nonpermeable Pr^{3+} was not able to interact with glyphosate inside the liposomes. All spectra in this figure were collected at pH 7.5.

stopped by adding 1 mL of 2 M NaOH. The samples were lyophilized and reconstituted in water. The water volume for reconstitution was decreased from 5 to 2 mL as glyphosate was consumed for glyphosate preconcentration to be within the working range of the isotope measurements (see below). The isotope ratio (expressed using the delta notation $\delta^{13}C$ in per mille (‰) relative to Vienna PeeDee Belemnite (V-PDB)) and the concentration of glyphosate were determined by liquid chromatography Isolink-isotope ratio mass spectrometry (LC-IRMS) (Thermo Fisher, Germany). The method used for carbon isotope analysis of glyphosate was modified from Kujawinski et al.[56] as follows: A mixed-phase Primesep 100 column 100 × 5.6 mm, 3 μm particle size (SIELC Technologies, USA) was used as stationary phase, and 2.5 mM phosphate buffer at pH 3.1 was used as mobile phase. Separation was achieved with 300 $\mu L \cdot min^{-1}$ isocratic flow. The injection volume was 25 μL. The reagents for chemical conversion to CO_2 at 99.9 °C were 1.5 M phosphoric acid and 0.84 M peroxodisulfate at a flow rate of 50 $\mu L \cdot min^{-1}$ each. The helium (grade 5.0) flow rate in the separation unit was set to 2.3 $mL \cdot min^{-1}$. The glyphosate concentration was determined with the area of the glyphosate CO_2 peak in the LC Isolink-IRMS chromatogram via external calibration with glyphosate standards in water (0.03, 0.06, 0.12, and 0.30 mM).

RESULTS AND DISCUSSION

Praseodymium(III) Ions Interact with Glyphosate As Well As the Liposome Surface. The liposome were of a uniform size with a hydrodynamic diameter of 204 ± 5 nm (median ± standard deviation, range: 194 nm to 239 nm). The median polydispersity index was 0.093 indicating a uniform and narrow size distribution of the individual liposome preparations. The near zero zeta potential of the liposomes composed of lipids bearing zwitterionic phosphatidylcholine headgroups[57] changed to +29 ± 6 mV upon $PrCl_3$ addition, because the strongly positively charged Pr^{3+} associated with the negatively charged phosphate group of POPC. Praseodymium(III) was added to produce a chemical environment outside the liposomes differing from that inside to allow glyphosate exchange across the membrane to be quantified. Indeed, addition of Pr^{3+} resulted in an interaction of glyphosate with the chemical shift agent which led to a position-specific downfield shift ($\Delta\delta_H$) of the glyphosate ^{1}H NMR signals. The chemical shift change produced by a 1 mM $PrCl_3$ solution was $\Delta\delta_H$ = 0.06 ppm for the $PO_3^{2-}-CH_2-NH_2^{+}-C\underline{H}_2-COO^{-}$ protons and $\Delta\delta_H$ = 0.16 ppm for the $PO_3^{2-}-C\underline{H}_2-NH_2^{+}-CH_2-COO^{-}$ protons in the ^{1}H NMR spectrum of glyphosate (Figure S1). The phosphorus peak was shifted downfield by $\Delta\delta_P$ = 1.29 ppm in the $^{31}P\{1H\}$ spectrum (Figure S1). The chemical shift change was strongest for the phosphorus peak and weakest for the protons adjacent to the carboxyl group which indicated that Pr^{3+} directly interacted with the negatively charged phosphate group and not with the negatively charged carboxyl group of the zwitterionic glyphosate.

Addition of Praseodymium(III) and Subsequent Peak Shape Analysis Quantified Chemical Exchange of Glyphosate. Subsequent addition of 0.5 mM Pr^{3+} to a glyphosate solution without liposomes moved the chemical shift of the collapsed singlet of the $PO_3^{2-}-C\underline{H}_2-NH_2^{+}-CH_2-COO^{-}$ protons downfield from 2.99 to 3.06 ppm. Interaction with the paramagnetic Pr^{3+} changes the local magnetic field, leading to the shift in frequency; the association/dissociation of Pr^{3+} and glyphosate produced line broadening (Figure 2B). We observed a similarly strong chemical shift change when adding Pr^{3+} to a glyphosate solution containing liposomes (Figure 2C). While the interaction of nonpermeable Pr^{3+} with glyphosate outside the liposomes influenced the chemical shift, the shift agent could not enter the liposomes as demonstrated by the unchanged chemical shift for glyphosate inside the liposomes. As a consequence, two distinct peaks appeared in the spectrum, and the glyphosate peak outside the liposomes was well-resolved from the peak inside. This indicated that the exchange was slow on the NMR time scale; that is, the ratio $k_{tr}/\Delta\delta_H$ is smaller than one ($k_{tr}/\Delta\delta_H < 1$), where k_{tr} is the apparent rate constant of exchange and $\Delta\delta_H$ is the chemical shift difference in ^{1}H NMR.[47] The glyphosate exchange across the liposome bilayer was fast enough, however, to lead to considerable line broadening, $\Delta\upsilon$, of the peak corresponding to glyphosate inside the liposomes. The line broadening ($\Delta\upsilon$) depends on the apparent rate constant of exchange according to eq 2[37] and ranged from $\Delta\upsilon$ = 2.6 Hz at neutral pH to $\Delta\upsilon$ = 40.8 Hz at pH 4.

DOI: 10.1021/acs.est.8b01004
Environ. Sci. Technol. 2018, 52, 7259−7268

$$\Delta\upsilon = \frac{k_{tr}}{\pi} \quad (2)$$

The glyphosate peaks inside the liposomes were fitted to determine the peak width prior to (υ_0) and after addition of $PrCl_3$ (υ_{ex}). The resultant line broadening $\Delta\upsilon = \upsilon_{ex} - \upsilon_0$ (Figure 2C) was used to calculate k_{tr} for each liposome preparation.

Glyphosate Permeation of Lipid Bilayers Depends Strongly on pH. Because k_{tr} strongly depends on the surface area and on the size of the liposomes, k_{tr} is not suitable to compare the chemical exchange of different liposome preparations and at different pH values. Therefore, Males and Herring derived the apparent permeation coefficient, P_{app} [m·s^{-1}], by including the inner liposome volume and the volume-to-surface ratio according to eq 3,[37] where d_{lip} is the diameter of the liposome and δ is the membrane thickness (4 nm); note that this membrane thickness δ should not be confused with the chemical shift δ_H (or δ_P) in the NMR spectrum or the $\delta^{13}C$ value. Our NMR approach is not subject to unstirred water layer effects (i.e., the permeation coefficient so determined reflects primarily diffusion across the lipid bilayer alone). The NMR experiments measured a dynamic exchange process under equilibrium conditions. The k_{tr} does, however, include a contribution from glyphosate diffusing a short distance through water to arrive at the lipid bilayer surface. We therefore refer to our rate constant of exchange as an apparent value and the permeation coefficient derived from it as an apparent permeation coefficient, P_{app}.

$$P_{app} = \frac{k_{tr}\cdot(d_{lip} - 2\delta)}{6} = \frac{\Delta\upsilon\cdot\pi\cdot(d_{lip} - 2\delta)}{6} \quad (3)$$

The permeation coefficient describes how rapidly glyphosate permeates a hypothetical two-dimensional POPC membrane sheet and was much higher than expected (Figure 3A). At circumneutral pH, the apparent permeation coefficient of glyphosate (double negatively charged, molecular weight (MW) = 167 g·mol^{-1}) P_{app} (pH 7.0) = 3.7 (±0.3) × 10^{-7} m·s^{-1} was considerably higher than that of maleate[46] (net dianion, MW = 114 g·mol^{-1}) and in the same range as the permeation coefficient of the polar, neutral serotonin species (MW = 176 g·mol^{-1}).[58] With decreasing pH, the permeation rate increased, with an apparent permeation coefficient of P_{app}(pH 4.1) = 4.2 (±0.1) × 10^{-6} m·s^{-1} at pH 4.1. The pH dependence correlated linearly with the average degree of ionization and thus the average charge of glyphosate (Figure 3B). The net charge of −2 (one positive and three negative charges) of glyphosate at neutral pH slowed passive membrane permeation. Protonation of the phosphate group at pH 4.1 reduced the net charge of glyphosate to −1 and, consequently, accelerated membrane permeation. This also indicates that the effect of Pr^{3+} on the measured permeation coefficient is negligible. If the change toward positive liposome surface potential due to Pr^{3+} addition (vide supra) facilitated permeation due to attraction of the strongly negatively charged glyphosate, the doubly negatively charged glyphosate species would permeate faster. However, the opposite is the case. Furthermore, two distinct glyphosate peaks appear in the NMR spectrum (vide supra), demonstrating that Pr^{3+} does not enter the liposomes together with glyphosate, which could lead to changed permeation characteristics. Therefore, we hypothesize that the zwitterionic structure of glyphosate facilitates glyphosate permeation, whereas the increased negative charge at neutral pH slowed passive permeation of glyphosate.

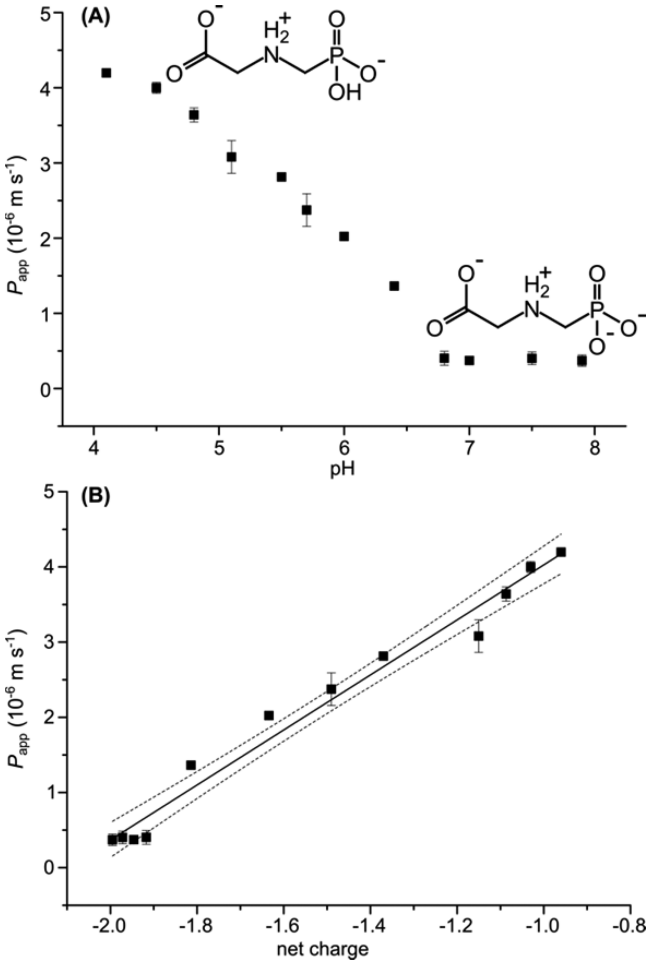

Figure 3. The pH dependence of the permeation coefficient P_{app} (black squares) correlated with the net charge of glyphosate. (A) P_{app} depended strongly on the pH of the liposome solution. The permeation at neutral pH (P_{app} (pH 7.0) = 3.7 (±0.3) × 10^{-7} m·s^{-1}) was 1 order of magnitude lower than at slightly acidic pH (P_{app} (pH 4.1) = 4.2 (±0.1) × 10^{-6} m·s^{-1}). (B) Permeation correlated with the ionization of glyphosate which can be explained by species-specific permeation coefficients for the net monoanion and net dianion. Both panels show the mean values with error bars denoting one standard deviation.

Membrane Permeation Can Lead to Considerable Glyphosate Uptake into Bacterial Cells. The entry of nonpolar pollutants into bacterial cells by passive permeation of the cell envelope is well recognized,[30,59] and charged, polar molecules like glyphosate are commonly assumed to be taken up almost exclusively by active transport or porin-assisted permeation.[60,61] Contrary to this expectation, in a liposome model system that lacked transporters or porins we observed membrane permeation coefficients for glyphosate in the same range as those for noncharged molecules (see above).[58] This observation suggests that passive membrane permeation of glyphosate mono- and dianions may provide sufficient influx into bacterial cells for the herbicide to serve as a phosphorus source. Glyphosate diffusion through water is fast compared to that through the lipid membrane.[62,63] The membrane therefore represents a significant diffusive barrier influences the rate the amount of substrate outside the bacteria is reduced via passive

DOI: 10.1021/acs.est.8b01004
Environ. Sci. Technol. 2018, 52, 7259−7268

membrane permeation at the rate $(dn_{out}/dt)_{permeation}$, where n_{out} denotes the number of moles of glyphosate outside the bacterial cell. This process is driven by the concentration gradient across the membrane and is defined by the linear exchange term in eq 4 as proposed by Males et al.[64]

$$\left(\frac{dn_{out}}{dt}\right)_{permeation} = -(k_{tr}K_{lip\text{-}w}[S_{out}]) + (k_{tr}K_{lip\text{-}w}[S_{in}]) \quad (4)$$

Here, $K_{lip\text{-}w}$ is the membrane lipid−water partition coefficient, and $[S_{out}]$ and $[S_{in}]$ are the glyphosate concentrations outside and inside the bacterial cell. The products $K_{lip\text{-}w}[S_{out}]$ and $K_{lip\text{-}w}[S_{in}]$ are the concentrations within the lipid membrane (outside and inside), respectively. With the definition of the diffusion coefficient across the membrane (lipid bilayer) D_{lip} (eq 5), the apparent rate constant of exchange (k_{tr}) can be calculated for a single bacterial cell by eq 6

$$D_{lip} = \frac{P_{app}\cdot\delta}{K_{lip\text{-}w}} \quad (5)$$

$$k_{tr} = \frac{D_{lip}\cdot A_{cell}}{\delta} = \frac{P_{app}\cdot A_{cell}}{K_{lip\text{-}w}} \quad (6)$$

where $A_{cell} \approx 3\ \mu m^2$ is the estimated surface area of one bacterial cell and δ is the membrane thickness (one 4 nm membrane in Gram-positive and two 4 nm thick membranes in Gram-negative bacteria). Together with eq 7, a term is obtained for the concentration gradient-dependent glyphosate influx into a single bacterial cell.

$$\left(\frac{dn_{out}}{dt}\right)_{cell\text{-}permeation} = -(P_{app}A_{cell}[S_{out}]) + (P_{app}A_{cell}[S_{in}]) \quad (7)$$

The glyphosate influx is at its maximum $(dn_{out}/dt)_{cell\text{-}permeation\text{-}max}$ when the concentration gradient is large ($[S_{in}] = 0$). We compared this maximum permeation rate with the glyphosate degradation rate of *Achromobacter sp.* MPS 12A described by Sviridov et al.[22] The glyphosate degradation rate of a single *Achromobacter sp.* MPS 12A cell $(dn/dt)_{deg\text{-}cell} = -1.4 \times 10^{-21}$ mol·s^{-1}·cell^{-1} at a concentration of 3 mM[22] was estimated by correlating the number of cells with the optical density OD_{600} and the bulk glyphosate degradation rate. While this correlation strongly depends on the strain and the growth conditions, the previously reported value of 8×10^8 cells·mL^{-1}·OD_{600}^{-1} provides a good first estimate.[65,66] The comparison showed that the calculated maximum membrane permeation rate at pH 7 $(dn_{out}/dt)_{cell\text{-}perm\text{-}max} = -1.9 \times 10^{-18}$ mol·s^{-1}·cell^{-1} was 2 orders of magnitude higher than the degradation rate. As a consequence, even though glyphosate has a net charge of −2 at pH 7, its passive membrane permeation is predicted to be fast enough to sustain bacterial transformation at the maximum degradation rate. This hypothesis clearly warrants further testing. If true, confirmation should be possible by (a) the observation of similarly rapid biodegradation per cell in a different strain and (b) applying compound-specific isotope fractionation as a diagnostic tool to observe the absence of mass transfer limitations directly. If permeation is indeed faster than enzymatic conversion, glyphosate molecules inside and outside the cell are expected to be in rapid equilibrium. Thus, glyphosate molecules enriched in heavy isotopes due to the enzymatic reaction in the cytosol will pass out of the cell into the bulk solution. This would lead to the isotope effect of the enzyme reaction being observable outside the cell, resulting in strong isotope fractionation during biodegradation. A new bacterium was, therefore, isolated from soil, and isotope fractionation was measured during glyphosate degradation.

Isolation and Glyphosate Degradation Activity of *Orchrobactrum sp.* FrEM. Repeated subculturing of an inoculum from soil samples in a medium containing 3 mM glyphosate as the sole phosphorus source resulted in the isolation of a bacterial strain with glyphosate-degrading activity. Glyphosate was used only as phosphorous source, consistent with Shushkova et al. how faced difficulties when using glyphosate as the sole carbon and phosphorus source for isolation.[67] The bacteria were rod-shaped as observed by light microscopy (Figure S2). Sequence alignment (BLAST) of the 16S rRNA showed a 99% homology with *Ochrobactrum anthropic*, *O. rhizosphaerae*, *O. pituitosum*, and *O. intermedium*, which all belong to the family of Brucellaceae in Alphaproteobacteria, and 70% homology with *Ochrobactrum hematophilum*. The strain was termed *Ochrobactrum sp.* FrEM (Figure S3). The fastest glyphosate degradation by *O. sp.* FrEM occurred after 4.5 days when the cell density was high ($OD_{600} \approx 0.8$). Within 12 h, the glyphosate concentration decreased from 104 to 55 mM equaling a maximum glyphosate degradation rate $(dn/dt)_{deg\text{-}cell} = -1.7 \times 10^{-21}$ mol·s^{-1}·cell^{-1} (Figure 4A) which was as high as that of *Achromobacter sp.* MPS 12A (see above).[22] Furthermore, just as for *Achromobacter sp.* MPS 12A, the calculated maximum membrane permeation rate at pH 7 $(dn_{out}/dt)_{cell\text{-}perm\text{-}max} = -7.5 \times 10^{-20}$ mol·s^{-1}·cell^{-1} at a concentration of 0.12 mM was larger than the degradation rate indicating that passive permeation of the cell envelope is likely not rate limiting for glyphosate biodegradation. We subsequently aimed to verify this hypothesis by compound-specific isotope fractionation analysis.

Carbon Isotope Fractionation Revealed Rapid Glyphosate Mass Transfer Across the Cell Wall. Glyphosate biodegradation by *O. sp.* FrEM (Figure 4A) was accompanied by significant carbon isotope fractionation. The $\delta^{13}C$ values of glyphosate increased from −28 (±0.5)‰ in the beginning to −19 (±0.5)‰ after 90% glyphosate conversion reflecting an enrichment of ^{13}C over ^{12}C. The corresponding enrichment factor $\varepsilon^{13}C = -4.5$ (±0.5)‰ was determined according to the Rayleigh equation (Figure 5 and eq 1). The primary apparent kinetic isotope effect, AKIE, a measure for the isotope effect at the reactive position, allows the direct comparison of isotope effects of different reactions and reactants and was calculated according to eq 8[68]

$$AKIE_{carbon} = \frac{1}{\frac{n}{x}\varepsilon^{13}C + 1} \quad (8)$$

where n denotes the total number of carbon atoms and x is the number of carbon atoms at the reactive position. With $n = 3$ and $x = 1$, the primary apparent kinetic isotope effect for glyphosate degradation (via breaking a single bond between carbon and phosphorus) was $AKIE_{carbon} = 1.014 \pm 0.003$, which is in the range of chemical reactions that involve breaking a single bond to a carbon atom.[68,69]

This suggests that if any additional rate-determining steps such as active transport[33] or slow passive membrane permeation[31] masked the enzymatic isotope fractionation, such an effect was small. As a consequence, we conclude that, indeed, glyphosate exchanged rapidly across the cell envelope

DOI: 10.1021/acs.est.8b01004
Environ. Sci. Technol. 2018, 52, 7259−7268

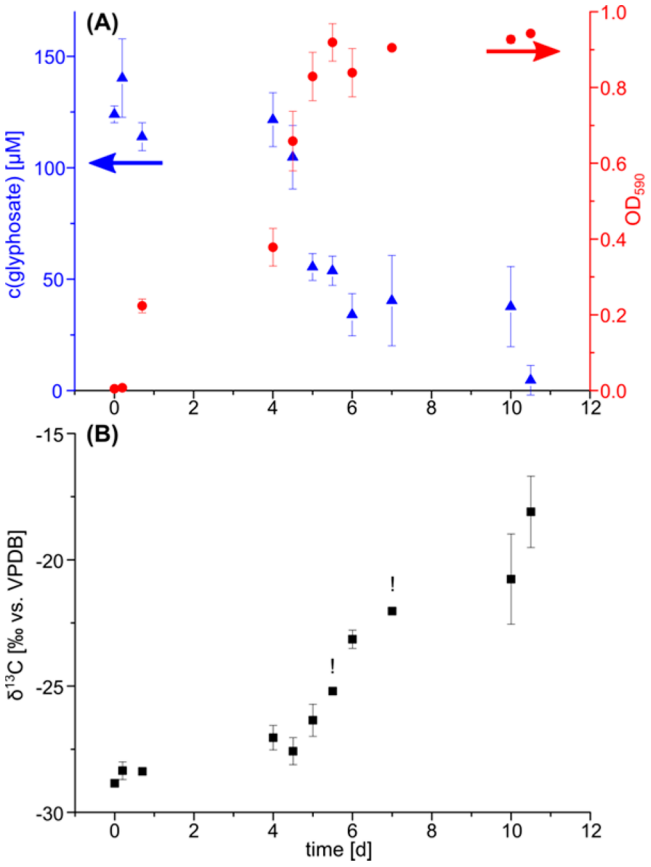

Figure 4. Glyphosate biodegradation was accompanied by growth and strong isotope fractionation. (A) Glyphosate degradation by *Ochrobactrum sp.* FrEM. Consumption of glyphosate (blue triangles) as source of phosphorus led to bacterial growth (red circles). (B) During this biodegradation, $^{13}C/^{12}C$ ratios of glyphosate increased, as indicated by less negative $\delta^{13}C$ values. All graphs show the mean and the error bars indicating the range of two biological replicates. The exclamation marks (!) above two isotope data points indicate that a reliable isotope value could be measured for only one biological replicate at the respective time points. Isotope values were measured in technical triplicates for each sample and are associated with an analytical uncertainty of ±0.3‰.

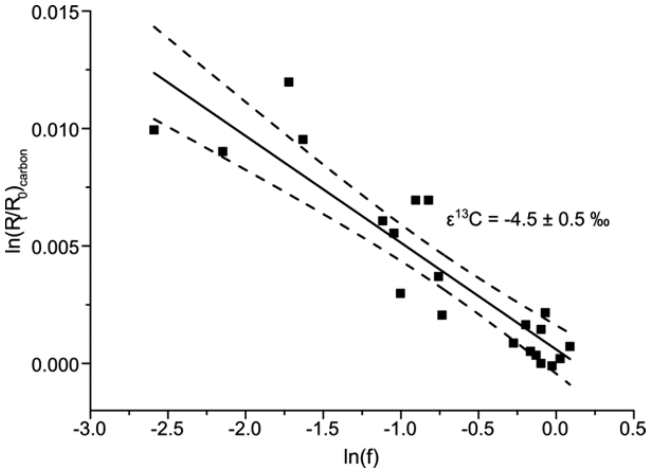

Figure 5. Pronounced isotope fractionation indicated rapid glyphosate exchange across the bacterial cell envelope. The carbon isotope fractionation factor ($\varepsilon^{13}C$ = −4.5 (±0.5)‰) was determined according to the Rayleigh equation (eq 1). The corresponding $AKIE_{carbon}$ = 1.014 ± 0.003 (see eq 8) was in the range of typical carbon isotope effects. This indicated that the enzymatic isotope fractionation was not masked by mass transfer limitations and that exchange of glyphosate across the cell envelope was comparatively rapid during bacterial degradation by *Ochrobactrum sp.* FrEM.

consistent with our hypothesis that passive permeation across the cell envelope may be an important, and until now underestimated, driver to facilitate biodegradation of glyphosate or other charged pollutants (C, N, and P sources). Future research should not only address the role of pH in the permeation of whole cells during biodegradation but also elucidate the possible role of transporters or porins (e.g., by studying isotope fractionation during glyphosate degradation in cell-free extracts of *O. sp.* FrEM or with liposomes containing the degrading enzyme).

Possibility of Mass Transfer Limitations at Low Concentrations in the Environment. While passive membrane permeation has previously been associated with nonpolar molecules, our results suggest that in addition to protein-assisted uptake (e.g., by active transporters[70,71] or assisted diffusion via porins[29,72]), charged species like glyphosate can enter bacterial cells by passive permeation of the cell membrane and that this can occur more rapidly than commonly thought. This can facilitate glyphosate biodegradation and lead to rapid turnover at high concentrations in water and soil.[10] A different situation must be considered, however, if the concentration gradient across the cell envelope is shallower, that is, than in our experiments. While the degradation-associated isotope fractionation was determined at high concentrations (>25 µM), the concentration in soil, groundwaters, and surface waters is much lower (<2 µM, <15 nM, and <0.5 µM, respectively).[18,73] We recently demonstrated that mass transfer across the cell membrane becomes rate-limiting for atrazine biodegradation at trace concentrations.[25] Similarly, at a glyphosate concentration of 1 µM, the calculated maximum membrane permeation rate is only $(dn_{out}/dt)_{cell\text{-}perm\text{-}max} = -6.5 \times 10^{-22}$ mol·s^{-1}·cell^{-1}, which is lower than the respective degradation rate per cell. At these concentrations, acceleration of cell wall transfer of glyphosate with high affinity active transporters may become necessary to boost biodegradation. Interestingly, Pipke et al. described such an active glyphosate transporter with an uptake rate of $(dn_{out}/dt)_{cell\text{-}transport} = -1.8 \times 10^{-21}$ mol·s^{-1}·cell^{-1} which is just in the range of observed glyphosate degradation rates.[74] However, its affinity constant K_M = 0.125 mM for glyphosate uptake is rather high, resulting in low transporter activity at trace concentrations. This increased mass transfer limitation at trace concentrations may cause biodegradation to stall and might explain the frequent detection of glyphosate in the environment.[17]

■ ASSOCIATED CONTENT

Supporting Information

The Supporting Information is available free of charge on the ACS Publications website at DOI: 10.1021/acs.est.8b01004.

A list of chemicals, media composition, strain isolation procedure, figures of the glyphosate spectra, micrograph of *Ochrobactrum sp.* FrEM, phylogenetic tree, LC-IRMS chromatogram, and a table summarizing spectra collection parameters (PDF)

DOI: 10.1021/acs.est.8b01004
Environ. Sci. Technol. 2018, 52, 7259−7268

AUTHOR INFORMATION

Corresponding Authors

*E-mail: m.elsner@tum.de; phone: +49 89 2180-78232 (M.E.).
*E-mail: joelpedersen@wisc.edu; phone: +1 608 263 4971 (J.A.P.).

ORCID

Joel A. Pedersen: 0000-0002-3918-1860
Martin Elsner: 0000-0003-4746-9052

Author Contributions

The manuscript was written through contributions of all authors. All authors have given approval to the final version of the manuscript.

Notes

The authors declare no competing financial interest.

ACKNOWLEDGMENTS

This work was funded by an ERC consolidator grant ("MicroDegrade", grant no. 616861) awarded by the European Research Council to M.E. The NMR instrumentation was supported by a generous gift from Paul J. and Margaret M. Bender to the Magnetic Resonance Facility in the Chemistry Department of the University of Wisconsin-Madison. J.A.P. gratefully acknowledges the support of the William A. Rothermel Bascom Professorship.

REFERENCES

(1) Franz, J. E.; Mao, M. K.; Sikorski, J. A. *Glyphosate: a unique global herbicide*; American Chemical Society: Washington, DC, 1997.
(2) Dill, G. M.; Sammons, R. D.; Feng, P. C. C.; Kohn, F.; Kretzmer, K.; Mehrsheikh, A.; Bleeke, M.; Honegger, J. L.; Farmer, D.; Wright, D.; Haupfear, E. A. Glyphosate: discovery, development, applications, and properties. In *Glyphosate Resistance in Crops and Weeds*; John Wiley & Sons, Inc.: New York, 2010; pp 1−33.
(3) Duke, S. O.; Powles, S. B. Glyphosate: a once-in-a-century herbicide. *Pest Manage. Sci.* **2008**, *64* (4), 319−325.
(4) Dill, G. M. Glyphosate-resistant crops: history, status and future. *Pest Manage. Sci.* **2005**, *61* (3), 219−224.
(5) Bøhn, T.; Cuhra, M.; Traavik, T.; Sanden, M.; Fagan, J.; Primicerio, R. Compositional differences in soybeans on the market: Glyphosate accumulates in roundup ready GM soybeans. *Food Chem.* **2014**, *153*, 207−215.
(6) Woodburn, A. T. Glyphosate: Production, pricing and use worldwide. *Pest Manage. Sci.* **2000**, *56* (4), 309−312.
(7) USGS. Estimated Annual Agricultural Pesticide Use; https://water.usgs.gov/nawqa/pnsp/usage/maps/show_map.php?year=2015&map=GLYPHOSATE&hilo=H&disp=Glyphosate (accessed 05.04.2018).
(8) Helander, M.; Saloniemi, I.; Saikkonen, K. Glyphosate in northern ecosystems. *Trends Plant Sci.* **2012**, *17* (10), 569−574.
(9) Relyea, R. A. The lethal impact of roundup on aquatic and terrestrial amphibians. *Ecological Applications* **2005**, *15* (4), 1118−1124.
(10) Giesy, J. P.; Dobson, S.; Solomon, K. R. Ecotoxicological risk assessment for roundup herbicide. In *Reviews of Environmental Contamination and Toxicology: Continuation of Residue Reviews*; Ware, G. W., Ed.; Springer New York: New York, NY, 2000; pp 35−120.
(11) Sullivan, T. P.; Sullivan, D. S. Vegetation management and ecosystem disturbance: Impact of glyphosate herbicide on plant and animal diversity in terrestrial systems. *Environ. Rev.* **2003**, *11* (1), 37−59.
(12) Mamy, L.; Gabrielle, B.; Barriuso, E. Comparative environmental impacts of glyphosate and conventional herbicides when used with glyphosate-tolerant and non-tolerant crops. *Environ. Pollut.* **2010**, *158* (10), 3172−3178.
(13) Firbank, L. G.; Forcella, F. Genetically modified crops and farmland biodiversity. *Science* **2000**, *289* (5484), 1481−1482.
(14) WHO. *IARC Monographs: Evaluation of Five Organophosphate Insecticides and Herbicides*; WHO: Geneva, 2015; Vol. *112*.
(15) Chang, E. T.; Delzell, E. Systematic review and meta-analysis of glyphosate exposure and risk of lymphohematopoietic cancers. *J. Environ. Sci. Health, Part B* **2016**, *51* (6), 402−434.
(16) Andreotti, G.; Koutros, S.; Hofmann, J. N.; Sandler, D. P.; Lubin, J. H.; Lynch, C. F.; Lerro, C. C.; De Roos, A. J.; Parks, C. G.; Alavanja, M. C.; Silverman, D. T.; Beane Freeman, L. E. Glyphosate use and cancer incidence in the agricultural health study. *JNCI: Journal of the National Cancer Institute* **2018**, *110*, 509.
(17) Mamy, L.; Barriuso, E.; Gabrielle, B. Environmental fate of herbicides trifluralin, metazachlor, metamitron and sulcotrione compared with that of glyphosate, a substitute broad spectrum herbicide for different glyphosate-resistant crops. *Pest Manage. Sci.* **2005**, *61* (9), 905−916.
(18) Battaglin, W. A.; Meyer, M. T.; Kuivila, K. M.; Dietze, J. E. Glyphosate and its degradation product ampa occur frequently and widely in u.s. Soils, surface water, groundwater, and precipitation. *J. Am. Water Resour. Assoc.* **2014**, *50* (2), 275−290.
(19) Horth, H.; Blackmore, K. *Survey of Glyphosate and Ampa in Groundwaters and Surface Waters in Europe*; No.: UC8073; WRc plc: Swindon, Wiltshire, United Kingdom, 2009; Vol. *2*.
(20) Ermakova, I.; Kiseleva, N.; Shushkova, T.; Zharikov, M.; Zharikov, G.; Leontievsky, A. Bioremediation of glyphosate-contaminated soils. *Appl. Microbiol. Biotechnol.* **2010**, *88* (2), 585−594.
(21) Pipke, R.; Amrhein, N. Degradation of the phosphonate herbicide glyphosate by *Arthrobacter atrocyaneus* ATCC 13752. *Appl. Environ. Microbiol.* **1988**, *54* (5), 1293−1296.
(22) Sviridov, A. V.; Shushkova, T. V.; Zelenkova, N. F.; Vinokurova, N. G.; Morgunov, I. G.; Ermakova, I. T.; Leontievsky, A. A. Distribution of glyphosate and methylphosphonate catabolism systems in soil bacteria *Ochrobactrum anthropi* and *Achromobacter* sp. *Appl. Microbiol. Biotechnol.* **2012**, *93* (2), 787−96.
(23) Borggaard, O. K.; Gimsing, A. L. Fate of glyphosate in soil and the possibility of leaching to ground and surface waters: A review. *Pest Manage. Sci.* **2008**, *64* (4), 441−456.
(24) Bosma, T. N. P.; Middeldorp, P. J. M.; Schraa, G.; Zehnder, A. J. B. Mass transfer limitation of biotransformation: Quantifying bioavailability. *Environ. Sci. Technol.* **1997**, *31* (1), 248−252.
(25) Ehrl, B. N.; Kundu, K.; Gharasoo, M.; Marozava, S.; Elsner, M. Rate limiting mass transfer in micropollutant degradation revealed by isotope fractionation. *Environ. Sci. Technol.*, submitted for publication.
(26) Sprankle, P.; Meggitt, W.; Penner, D. Adsorption, mobility, and microbial degradation of glyphosate in the soil. *Weed Science* **1975**, *23*, 229−234.
(27) Button, D. K. Kinetics of nutrient-limited transport and microbial growth. *Microbiol. Rev.* **1985**, *49*, 270−297.
(28) Ferenci, T.; Robert, K. P. Bacterial physiology, regulation and mutational adaptation in a chemostat environment. In *Advances in Microbial Physiology*; Academic Press: New York, 2008; Vol. *53*, pp 169−315.
(29) Delcour, A. H. Outer membrane permeability and antibiotic resistance. *Biochim. Biophys. Acta, Proteins Proteomics* **2009**, *1794* (5), 808−816.
(30) Parales, R. E.; Ditty, J. L. Substrate transport. In *Handbook of Hydrocarbon and Lipid Microbiology*; Timmis, K. N., Ed.; Springer Berlin Heidelberg: Berlin, Heidelberg, 2010; pp 1545−1553.
(31) Ehrl, B. N.; Gharasoo, M.; Elsner, M. Isotope fractionation pinpoints membrane permeability as a barrier to atrazine biodegradation in gram-negative *Polaromonas* sp. Nea-C. *Environ. Sci. Technol.* **2018**, *52* (7), 4137−4144.
(32) Wick, L. M.; Quadroni, M.; Egli, T. Short- and long-term changes in proteome composition and kinetic properties in a culture of *Escherichia coli* during transition from glucose-excess to glucose-limited growth conditions in continuous culture and vice versa. *Environ. Microbiol.* **2001**, *3* (9), 588−599.

DOI: 10.1021/acs.est.8b01004
Environ. Sci. Technol. 2018, 52, 7259−7268

(33) Qiu, S.; Gözdereliler, E.; Weyrauch, P.; Lopez, E. C. M.; Kohler, H.-P. E.; Sørensen, S. R.; Meckenstock, R. U.; Elsner, M. Small $^{13}C/^{12}C$ fractionation contrasts with large enantiomer fractionation in aerobic biodegradation of phenoxy acids. *Environ. Sci. Technol.* **2014**, *48* (10), 5501−5511.
(34) Beate, B. I.; Sigg, L. Chemical speciation of organics and of metals at biological interphases. In *Physicochemical Kinetics and Transport at Biointerfaces*; Hermann, P.; Van Leeuwen, W. K., Ed.; Wiley: New York, 2004; Vol. *9*, pp 205−269.
(35) Wohnsland, F.; Faller, B. High-throughput permeability pH profile and high-throughput alkane/water log P with artificial membranes. *J. Med. Chem.* **2001**, *44* (6), 923−930.
(36) Passeleu-Le Bourdonnec, C.; Carrupt, P.-A.; Scherrmann, J. M.; Martel, S. Methodologies to assess drug permeation through the blood−brain barrier for pharmaceutical research. *Pharm. Res.* **2013**, *30* (11), 2729−2756.
(37) Males, R. G.; Herring, F. G. A ^{1}H-NMR study of the permeation of glycolic acid through phospholipid membranes. *Biochim. Biophys. Acta, Biomembr.* **1999**, *1416* (1−2), 333−338.
(38) Naderkhani, E.; Vasskog, T.; Flaten, G. E. Biomimetic PVPA in vitro model for estimation of the intestinal drug permeability using fasted and fed state simulated intestinal fluids. *Eur. J. Pharm. Sci.* **2015**, *73*, 64−71.
(39) Lande, M. B.; Donovan, J. M.; Zeidel, M. L. The relationship between membrane fluidity and permeabilities to water, solutes, ammonia, and protons. *J. Gen. Physiol.* **1995**, *106* (1), 67−84.
(40) Dietrich, C.; Bagatolli, L. A.; Volovyk, Z. N.; Thompson, N. L.; Levi, M.; Jacobson, K.; Gratton, E. Lipid Rafts Reconstituted in Model Membranes. *Biophys. J.* **2001**, *80* (3), 1417−1428.
(41) Xlang, T.-X.; Anderson, B. D. Development of a combined NMR paramagnetic ion-induced line-broadening/dynamic light scattering method for permeability measurements across lipid bilayer membranes. *J. Pharm. Sci.* **1995**, *84* (11), 1308−1315.
(42) Russell, N. J.; Fukunaga, N. A comparison of thermal adaptation of membrane lipids in psychrophilic and thermophilic bacteria. *FEMS Microbiol. Lett.* **1990**, *75* (2−3), 171−182.
(43) Vanounou, S.; Pines, D.; Pines, E.; Parola, A. H.; Fishov, I. Coexistence of domains with distinct order and polarity in fluid bacterial membranes. *Photochem. Photobiol.* **2002**, *76* (1), 1−11.
(44) Epand, R. M.; Epand, R. F. Lipid domains in bacterial membranes and the action of antimicrobial agents. *Biochim. Biophys. Acta, Biomembr.* **2009**, *1788* (1), 289−294.
(45) Vollmer, W.; Blanot, D.; De Pedro, M. A. Peptidoglycan structure and architecture. *FEMS Microbiology Reviews* **2008**, *32* (2), 149−167.
(46) Prestegard, J. H.; Cramer, J. A.; Viscio, D. B. Nuclear magnetic resonance determinations of permeation coefficients for maleic acid in phospholipid vesicles. *Biophys. J.* **1979**, *26* (3), 575−584.
(47) Millet, O.; Loria, J. P.; Kroenke, C. D.; Pons, M.; Palmer, A. G. The static magnetic field dependence of chemical exchange line-broadening defines the nmr chemical shift time scale. *J. Am. Chem. Soc.* **2000**, *122* (12), 2867−2877.
(48) Melander, L.; Saunders, W. H. *Reaction Rates of Isotopic Molecules*; John Wiley: New York, 1980; p 331.
(49) Hoefs, J. Theoretical and Experimental Principles. In *Stable Isotope Geochemistry*, 3rd ed.; Wyllie, P. J., Ed.; Springer-Verlag: Chicago, 1987; pp 1−25.
(50) Schmidt, H. L. Fundamentals and systematics of the non-statistical distributions of isotopes in natural compounds. *Naturwissenschaften* **2003**, *90* (12), 537−552.
(51) Thullner, M.; Kampara, M.; Richnow, H. H.; Harms, H.; Wick, L. Y. Impact of bioavailability restrictions on microbially induced stable isotope fractionation. 1. Theoretical calculation. *Environ. Sci. Technol.* **2008**, *42* (17), 6544−6551.
(52) Kampara, M.; Thullner, M.; Richnow, H. H.; Harms, H.; Wick, L. Y. Impact of bioavailability restrictions on microbially induced stable isotope fractionation. 2. Experimental evidence. *Environ. Sci. Technol.* **2008**, *42* (17), 6552−6558.
(53) Thullner, M.; Fischer, A.; Richnow, H. H.; Wick, L. Y. Influence of mass transfer on stable isotope fractionation. *Appl. Microbiol. Biotechnol.* **2013**, *97* (2), 441−452.
(54) MacDonald, R. C.; MacDonald, R. I.; Menco, B. P. M.; Takeshita, K.; Subbarao, N. K.; Hu, L.-R. Small-volume extrusion apparatus for preparation of large, unilamellar vesicles. *Biochim. Biophys. Acta, Biomembr.* **1991**, *1061* (2), 297−303.
(55) Hope, M. J.; Bally, M. B.; Webb, G.; Cullis, P. R. Production of large unilamellar vesicles by a rapid extrusion procedure. Characterization of size distribution, trapped volume and ability to maintain a membrane potential. *Biochim. Biophys. Acta, Biomembr.* **1985**, *812* (1), 55−65.
(56) Kujawinski, D. M.; Wolbert, J. B.; Zhang, L.; Jochmann, M. A.; Widory, D.; Baran, N.; Schmidt, T. C. Carbon isotope ratio measurements of glyphosate and AMPA by liquid chromatography coupled to isotope ratio mass spectrometry. *Anal. Bioanal. Chem.* **2013**, *405* (9), 2869−2878.
(57) Moncelli, M. R.; Becucci, L.; Guidelli, R. The intrinsic pK_a values for phosphatidylcholine, phosphatidylethanolamine, and phosphatidylserine in monolayers deposited on mercury electrodes. *Biophys. J.* **1994**, *66* (6), 1969−1980.
(58) Viscio, D. B.; Prestegard, J. H. NMR studies of 5-hydroxytryptamine transport through large unilamellar vesicle membranes. *Proc. Natl. Acad. Sci. U. S. A.* **1981**, *78* (3), 1638−1642.
(59) Endo, S.; Escher, B. I.; Goss, K.-U. Capacities of membrane lipids to accumulate neutral organic chemicals. *Environ. Sci. Technol.* **2011**, *45* (14), 5912−5921.
(60) Kallimanis, A.; Frillingos, S.; Drainas, C.; Koukkou, A. I. Taxonomic identification, phenanthrene uptake activity, and membrane lipid alterations of the PAH degrading *Arthrobacter* sp. strain Sphe3. *Appl. Microbiol. Biotechnol.* **2007**, *76* (3), 709−717.
(61) Kell, D. B.; Dobson, P. D.; Oliver, S. G. Pharmaceutical drug transport: the issues and the implications that it is essentially carrier-mediated only. *Drug Discovery Today* **2011**, *16* (15−16), 704−714.
(62) Culbertson, C. T.; Jacobson, S. C.; Michael Ramsey, J. Diffusion coefficient measurements in microfluidic devices. *Talanta* **2002**, *56* (2), 365−373.
(63) Worch, E. A new equation for the calculation of diffusion coefficients for dissolved substances. *Vom Wasser* **1993**, *81*, 289−297.
(64) Males, R. G.; Phillips, P. S.; Herring, F. G. Equations describing passive transport through vesicular membranes. *Biophys. Chem.* **1998**, *70* (1), 65−74.
(65) Volkmer, B.; Heinemann, M. Condition-dependent cell volume and concentration of *Escherichia coli* to facilitate data conversion for systems biology modeling. *PLoS ONE* **2011**, *6* (7), e23126.
(66) Kopinke, F.-D.; Georgi, A.; Roland, U. Isotope fractionation in phase-transfer processes under thermodynamic and kinetic control − Implications for diffusive fractionation in aqueous solution. *Sci. Total Environ.* **2018**, *610−611* (Supplement C), 495−502.
(67) Shushkova, T. V.; Ermakova, I. T.; Sviridov, A. V.; Leontievsky, A. A. Biodegradation of glyphosate by soil bacteria: Optimization of cultivation and the method for active biomass storage. *Microbiology* **2012**, *81* (1), 44−50.
(68) Elsner, M.; Zwank, L.; Hunkeler, D.; Schwarzenbach, R. P. A new concept linking observable stable isotope fractionation to transformation pathways of organic pollutants. *Environ. Sci. Technol.* **2005**, *39* (18), 6896−6916.
(69) Mancini, S. A.; Hirschorn, S. K.; Elsner, M.; Lacrampe-Couloume, G.; Sleep, B. E.; Edwards, E. A.; SherwoodLollar, B. Effects of trace element concentration on enzyme controlled stable isotope fractionation during aerobic biodegradation of toluene. *Environ. Sci. Technol.* **2006**, *40* (24), 7675−7681.
(70) Muller, R. H.; Hoffmann, D. Uptake kinetics of 2,4-dichlorophenoxyacetate by *Delftia acidovorans* MC1 and derivative strains: Complex characteristics in response to pH and growth substrate. *Biosci., Biotechnol., Biochem.* **2006**, *70* (7), 1642−1654.
(71) Nichols, N. N.; Harwood, C. S. PcaK, a high-affinity permease for the aromatic compounds 4-hydroxybenzoate and protocatechuate from *Pseudomonas putida*. *J. Bacteriol.* **1997**, *179* (16), 5056−61.

DOI: 10.1021/acs.est.8b01004
Environ. Sci. Technol. 2018, 52, 7259−7268

(72) Button, D. K.; Robertson, B.; Gustafson, E.; Zhao, X. M. Experimental and theoretical bases of specific affinity, a cytoarchitecture-based formulation of nutrient collection proposed to supercede the Michaels-Menten paradigm of microbial kinetics. *Appl. Environ. Microbiol.* **2004**, *70* (9), 5511−5521.
(73) Sanchis, J.; Kantiani, L.; Llorca, M.; Rubio, F.; Ginebreda, A.; Fraile, J.; Garrido, T.; Farre, M. Determination of glyphosate in groundwater samples using an ultrasensitive immunoassay and confirmation by on-line solid-phase extraction followed by liquid chromatography coupled to tandem mass spectrometry. *Anal. Bioanal. Chem.* **2012**, *402* (7), 2335−2345.
(74) Pipke, R.; Schulz, A.; Amrhein, N. Uptake of Glyphosate by an *Arthrobacter* sp. *Appl. Environ. Microbiol.* **1987**, *53* (5), 974−978.

DOI: 10.1021/acs.est.8b01004
Environ. Sci. Technol. 2018, 52, 7259−7268